Marine and freshwater micropearls:

biomineralization producing strontium-rich amorphous calcium carbonate inclusions is widespread in the genus *Tetraselmis* (Chlorophyta)

Preprint version

Agathe Martignier[1], Montserrat Filella[2], Kilian Pollok[3], Michael Melkonian[4], Michael Bensimon[5], François Barja[6], Falko Langenhorst[3], Jean-Michel Jaquet[1], Daniel Ariztegui[1]

[1]Department of Earth Sciences, University of Geneva, Geneva, 1205, Switzerland
[2]Department F.-A. Forel, University of Geneva, Geneva, 1205, Switzerland
[3]Institute of Geosciences, Friedrich Schiller University Jena, Jena, 07745, Germany
[4]Botany Department, Cologne Biocenter, University of Cologne, Cologne, 50674, Germany
[5]EPFL ENAC IIE GR-CEL IsoTraceLab, EPFL, Lausanne, 1015 Switzerland
[6]Microbiology Unit, University of Geneva, Geneva, 1205, Switzerland

Correspondence to: Agathe Martignier (agathe.martignier@unige.ch)

Abstract. The genus *Tetraselmis* (Chlorophyta) includes more than 30 species of unicellular micro-algae that have been widely studied since the description of the first species in 1878. *Tetraselmis cordiformis* (presumably the only freshwater species of the genus) was discovered recently to form intracellular mineral inclusions, called micropearls, which had been previously overlooked. These non-skeletal intracellular inclusions of hydrated amorphous calcium carbonates (ACC) were first described in Lake Geneva (Switzerland) and are the result of a novel biomineralization process.

The present study shows that many *Tetraselmis* species share this biomineralization capacity: 10 species out of the 12 tested contained micropearls, including *T. chui*, *T.convolutae*, *T.levis*, *T. subcordiformis*, *T. suecica* and *T. tetrathele*. Our results indicate that micropearls are not randomly distributed inside the *Tetraselmis* cells, but are located preferentially under the plasma membrane and seem to form a definite pattern, which differs between species. In *Tetraselmis* cells, the biomineralization process seems to systematically start with a rod-shaped nucleus and results in an enrichment of the micropearls in strontium over calcium (the Sr/Ca ratio is up to 219 times higher in the micropearls than in the surrounding water or growth medium). This concentrating capacity varies from one species to the other, which might be of interest for possible bioremediation techniques regarding radioactive ^{90}Sr water pollution.

The *Tetraselmis* species forming micropearls live in various habitats, indicating that this novel biomineralization process can take place in different environments (marine, brackish and freshwater) and is therefore a widespread phenomenon.

1 Introduction

Micropearls are intracellular, non-skeletal mineral inclusions, consisting of hydrated amorphous calcium carbonates (ACC), frequently enriched in alkaline-earth elements (*e.g.* Sr or Ba). They typically display internal oscillatory zonation (Jaquet et al., 2013; Martignier et al., 2017), which is due to variations of the Ba/Ca or Sr/Ca ratios. Until now, this type of biomineralization process had been observed only in two freshwater organisms. One of them is the unicellular green alga *Tetraselmis cordiformis* (Chlorodendrophyceae, Chlorophyta) producing micropearls enriched in Sr. Since its first description in 1878 (Stein, 1878), the genus *Tetraselmis* has been well studied by biologists, because several species are economically important due to their high nutritional value and ease of culture (Hemaiswarya et al., 2011). *Tetraselmis* species are used extensively as aquaculture feed (Azma et al., 2011; Lu et al., 2017; Park and Hur, 2000; Zittelli et al., 2006) and some have been suggested as potential producers of biofuels (Asinari di San Marzano et al., 1981; Grierson et al., 2012; Lim et al., 2012; Montero et al., 2011; Wei et al., 2014). They have also served as models in algal research (Douglas, 1983; Gooday, 1970; Kirst, 1977; Marin et al., 1993; Melkonian, 1979; Norris et al., 1980; Regan, 1988; Salisbury et al., 1984). However, mineral inclusions had never been described in these microorganisms until the recent observation of micropearls in *Tetraselmis cordiformis* (Martignier et al., 2017). The fact that this new physiological trait had gone unnoticed is puzzling, especially as *Tetraselmis cordiformis* is the type species of the genus. This can probably be explained by the translucence of the micropearls under the optical microscope and their great sensitivity to pH variations, leading to their alteration or dissolution during most sample preparation techniques (Martignier et al., 2017).

Tetraselmis cordiformis is presumably the only freshwater species among the 33 species currently accepted taxonomically in the genus *Tetraselmis* (Guiry and Guiry, 2018). This genus has a cell wall formation process that is unique among green algae: the cells synthetize small non-mineralized scales in the Golgi apparatus, which are exocytosed through Golgi-derived secretory vesicles to form a solid wall (theca) composed of fused scales (Becker et al., 1994; Domozych, 1984; Manton and Parke, 1965). The motile cells of *Tetraselmis* have four scale-covered flagella, which emerge from an anterior (or apical) depression of the cell (Manton and Parke, 1965). Several *Tetraselmis* species (e.g. *T. subcordiformis*) have been mentioned as potential candidates for radioactive Sr bioremediation due to their high Sr absorption capacities (Fukuda et al., 2014; Li et al., 2006) but the precise process by which these microorganisms concentrate this element had never been determined before. Regarding their habitat, most *Tetraselmis* species are free-living (planktonic or benthic) (Norris et al., 1980) although some species live in specialized habitats, for example as endosymbiont in flatworms (Parke and Manton, 1967; Trench, 1979; Venn et al., 2008). The present study investigates twelve species of the genus *Tetraselmis*, including the freshwater *Tetraselmis cordiformis*, with the objective of understanding whether the biomineralization process leading to the formation of micropearls is common to the whole genus or is restricted to *T. cordiformis*. Species living in contrasting environments have been selected to evaluate also if the formation of micropearls is linked to their habitat. Each species is represented by one or several strains, obtained from public algal culture collections. The micropearls were imaged by scanning electron microscopy (SEM), and their composition measured by energy-dispersive X-ray spectroscopy (EDXS). The inner structure and chemical composition of micropearls in three different species were studied by transmission electron microscopy (TEM) on focused ion beam (FIB) cross sections.

2 Samples and Methods

2.1 Origin of the samples and pre-treatment methods

Culture samples of 12 different *Tetraselmis* species were obtained from three different algal culture collections and were grown in different media (Table 1). The recipe of each growth medium is available on the website of the respective culture collections. A single strain of each species was studied, except for *T. chui* and *T. tetrathele* (2 strains) as well as *T. cordiformis* (3 strains). Table 1 lists the strain names.

Samples for microscopic observation were prepared directly after the organisms' arrival in our laboratory: small portions of the culture (without any change of the original medium) were filtered under moderate vacuum (-20 to -30 kPa) on polycarbonate filter membranes with 0.2, 1 or 2 µm pore sizes. Volumes filtered (variable depending on culture concentration) were recorded. Species issued from SAG (Sammlung von Algenkulturen - University of Göttingen, Germany) were grown on agar and, therefore, cultures had to be diluted just before filtration. Filter membranes were dried in the dark at room temperature after filtration. A total of 458 micropearls were analysed by EDXS.

2.2 Water chemistry measurements

Elemental composition of each culture medium was measured at the IsoTraceLab (EPFL, Lausanne, Switzerland), except for the ES medium for which we could not obtain a sample. Blank samples of MilliQ water were embottled at the same time as growing medium samples and measured in the same way (Table S2 and Fig. S4). Barium and Sr were measured by Inductively Coupled Plasma Sector Field Mass Spectrometry (ICP-SFMS) using a Finnigan™ Element2 High Performance High Resolution ICP-MS model. The mass resolution was set to 500 to increase analytical sensitivity. Calibration standards were prepared through successive dilutions in cleaned Teflon bottles, of 0.1g l^{-1} ICPMS stock solutions (TechLab France). Suprapur® grade nitric acid (65% Merck) was used for the acidification in the preparation of standards. Ultrapure water was produced using Milli-Q® Ultrapure Water System (Millipore, Bedford, USA). Rhodium was used as Internal Standard (IS) for samples and standards to correct signal drift.

At this resolution mode, the sensitivity was less than $1.2x10^6$ cps/ppb of ^{115}In. The measurement repeatability expressed in terms of RSD was better than 5%. The accuracy of the method was tested using a home-made standard solution containing 5.0 ng l^{-1}, used as a reference. Accuracy was better than 5%. The detection limits obtained for Sr and Ba was around 100 ng l^{-1} under these experimental conditions.

2.3 Scanning electron microscopy (SEM) and EDXS analysis

Small portions of the dried filters were mounted on aluminium stubs with double-sided conductive carbon tape and then coated with gold coating (ca. 10 nm) by low vacuum sputter coating. A JEOL JSM 7001F Scanning Electron Microscope (Department of Earth Sciences, University of Geneva, Switzerland), equipped with an EDXS detector (model EX-94300S4L1Q; JEOL), was used to perform EDXS analyses and to obtain images of the dried samples. Semi-quantitative results were obtained using the ZAF correction method. Samples were imaged with backscattered electrons. This method allows to clearly locate the micropearls inside the organisms, thanks to the high difference of mean atomic numbers between the micropearls and the surrounding organic matter. EDXS measurements were acquired with settings of 15 kV accelerating voltage, a beam current of ~7 nA and acquisition times of 30 seconds. Semi-quantitative EDXS analyses of elemental concentrations were made without taking carbon, nitrogen and oxygen into account. EDXS results are all presented as mol%.

2.4 Focused ion beam (FIB) preparation

Electron-transparent lamellae for TEM were prepared with a FIB-SEM workstation (FEI Quanta 3D FEG at the Institute of Geosciences, Friedrich Schiller University Jena, Germany). The cells were previously selected based on SEM imaging. To protect the sample, a platinum strap of 15 to 30 µm length, ~3 µm width, and ~3 µm high was deposited on the cell during lamella preparation, via ion-beam induced deposition using the Gas Injection System (GIS). Stepped trenches were prepared on both sides of the Pt straps by Ga+ ion beam sputtering. This operation was performed at 30 keV energy and 3 to 5 nA beam current.

The resulting lamellae were then thinned to approximately 1 μm thickness by using sequentially lower beam currents at 30 keV energy (starting at 1 nA and ending at 0.5 or 0.3 nA). The position of the lamellae was chosen to include a maximum of micropearl cross-sections. An internal micromanipulator with tungsten needle was used to lift-out the pre-thinned lamellae and to transfer them to a copper grid.

Final thinning of the sample to electron transparency (~100 to 200 nm) was carried out on both sides of the lamellae by using sequentially lower beam currents (300 to 50 pA at 30 keV energy). The lamellae underwent only grazing incidence of the ion beam at this stage of the preparation. This allows to minimize ion beam damage and surface implantation of Ga. The thinning progress was observed with SEM imaging of the lamellae at 52°. Electron beam damage was further supressed by using low electron currents and limiting electron imaging to a strict minimum.

2.5 Transmission electron microscopy (TEM)

TEM investigations were conducted with a FEI Tecnai G2 FEG transmission electron microscope operating at 200kV. In order to document the structural state of micropearls in their pristine undamaged form, selected-area electron diffraction (SAED) patterns were taken directly at the beginning of the TEM session with a broad beam. Scanning TEM (STEM) images were then acquired using a High Angle Annular Dark Field (HAADF) STEM detector (Fischione) with a camera length of 80 mm. EDXS measurements were performed with a X-MaxN 80T SDD EDXS system (Oxford). EDXS spectra and maps were recorded in scanning TEM mode. The semi-quantitative calculation of the concentrations (including C) was obtained using the Cliff-Lorimer method using pre-calibrated k-factors and an absorption correction integrated into the Oxford software. The absorption correction is based on the principle of electroneutrality, taking into account the valence states and concentrations of cations and oxygen anions. Oxygen is thereby assumed to possess a stoichiometric concentration.

3 Results

3.1 Micropearls in *Tetraselmis* species

SEM observations of twelve different species of *Tetraselmis* (culture strains) show that ten of them contained mineral inclusions (Fig. 1, Table 1). No mineral inclusions were observed in *T. ascus* and *T. marina*. Since TEM analyses confirmed that these inclusions comply with the definition of micropearls given in Martignier et al. (2017) (see Sect. 4.1), they will be named “micropearls” hereafter.

The general shape of the micropearls in the marine species is elongated, resembling rice grains (Fig. 1 except 1d), while it is spherical in *T. cordiformis* (the only freshwater species of this study) (Fig. 1d). The micropearls’ size and shape differ among species. Sizes vary between 0.4 to 1.2 μm in length. Detailed values for each species are given in Table 1.

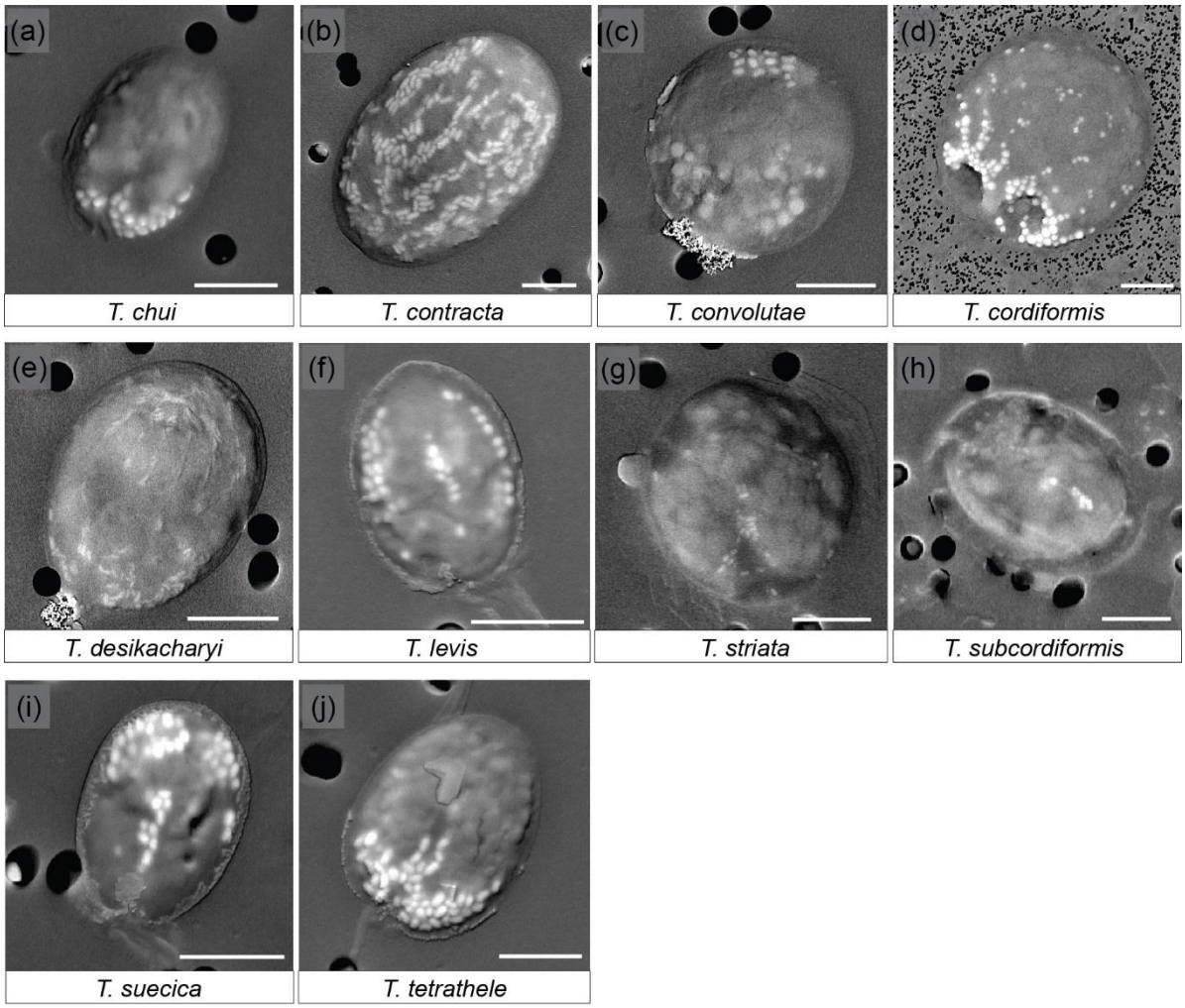

Figure 1: SEM images of ten *Tetraselmis* species containing micropearls at the time of observation.

Backscattered electron images of dried samples. The micropearls appear in white or light grey against the darker organic matter, as elongated shapes, except for *T. cordiformis* (d), where they are spherical. The larger and slightly darker inclusions are polyphosphates (c, g). Pores of the filters are visible as black circles in the background (2 μm of diameter except for (d): 0.2 μm). Scale bars: 5μm.

Micropearls do not seem to be randomly distributed inside the cells, but rather show a definite location in most species (Figs 1 and S1). Moreover, for a given species, most cells present a similar micropearl arrangement. Exceptions are cells that were damaged during sample preparation. Filtration or freshwater rinsing, for example, can disrupt the micropearl distribution pattern (Fig. S2).

In some strains, the micropearls are mostly aggregated at the one side of the cell, with "pointed" tips appearing at the center of the cell and on both sides, resulting in a "trident" shape. This is the case of *T. chui*, *T. suecica* and *T. tetrathele* (Figs 1a, 1i, 1j). *T. striata* shows a similar central micropearl distribution, but the lateral points of the "trident" are absent (Fig. 1g), possibly

due to poorly developed micropearls at the time of observation. In *T. suecica* the central micropearl alignment is generally longer and not necessarily connected to the apical aggregate (Fig. 1i). *T. levis* (Fig. 1f) also shows a similar arrangement, but the aggregate is missing, leaving the micropearls to form three longitudinal alignments (meridians). Altogether, *T. chui*, *T. levis*, *T. suecica* and *T. tetrathele* present patterns with an approximately similar trimerous radial organization (although a tetramerous symmetry cannot be totally excluded as dried samples do not allow a definite judgement). Observations seem to indicate that, in most species, the micropearl aggregate is located at the apical side of the cell (near the apical depression from which the four flagella emerge) (Figs S1) except for *T. suecica* and *T. convolutae* where the micropearls aggregate at the distal side of the cell (Figs S1, 1c and 1i). However, the low number of preserved flagella in dried samples allowed only for few confirmed observations. In *T. convolutae* (Fig. 1c), the micropearls form a small aggregate at the basal extremity of the cell, while larger polyphosphate inclusions gather at the opposite (apical) side.

A different and interesting organization of the micropearls is displayed by both *T. desikacharyi* (Fig. 1e) and *T. contracta* (Fig. 1b). An apical aggregate of micropearls is generally present, while other micropearls form regularly spaced meridians, which, in *T. contracta*, extend from the apical pole towards the basal part of the cell (Figs 1b and S1). These meridians are not well expressed in all cells but, when they are clearly visible, there seems to be around eight or ten of them inside the cell. When well preserved, the micropearl organization in *T. cordiformis* also shows multiple micropearl alignments which depart from a well-developed apical aggregate, although the alignments are generally well arranged only close to the aggregate and the size of micropearls decreases quickly towards the basal end of the cell (Fig. 1d). Finally, samples observed in this study did not allow us to state if there is a definite distribution of the micropearls in *T. subcordiformis* (Figs 1h and S1).

Polyphosphate inclusions are frequently observed in *Tetraselmis* species. Their distribution seems to be random except in *T. convolutae* (Fig. 1c). Aggregates of small iron oxide minerals were frequently observed in dried samples at one extremity of *T. desikacharyi* and *T. convolutae* (Figs 1c and 1e) – probably at the apical extremity.

In order to compare our results with members of another genus, we also analyzed other flagellate organisms (e.g. *Chlamydomonas reinhardtii* and *Chlamydomonas intermedia*) obtained from algal culture collections (Table 1). No calcium carbonate inclusions were observed in these cells. Thorough observation of samples from Lake Geneva confirms that most flagellates do not produce micropearls. This biomineralization process seems to be exclusive of a limited number of organisms.

3.2 TEM observation of FIB-cut cross-sections of micropearls

FIB-cut cross-sections of micropearls produced by *T. chui* and *T. suecica* are shown in Fig. 2, where they are compared to a similar section in a cell of the freshwater species *T. cordiformis* sampled in a natural environment (Lake Geneva). The choice of *T. chui* and *T. suecica* for FIB-processing and TEM observation was based on the size of the micropearls and on their strong concentration in Sr. Both features were considered to favour the observation of compositional zonation, as observed in our previous study (Martignier et al., 2017). A FIB-cut was also performed in a *Tetraselmis contracta* cell. This result is shown separately in Fig. 3, because the very good conservation of the organic matter in this sample allows the simultaneous observation of other intracellular constituents.

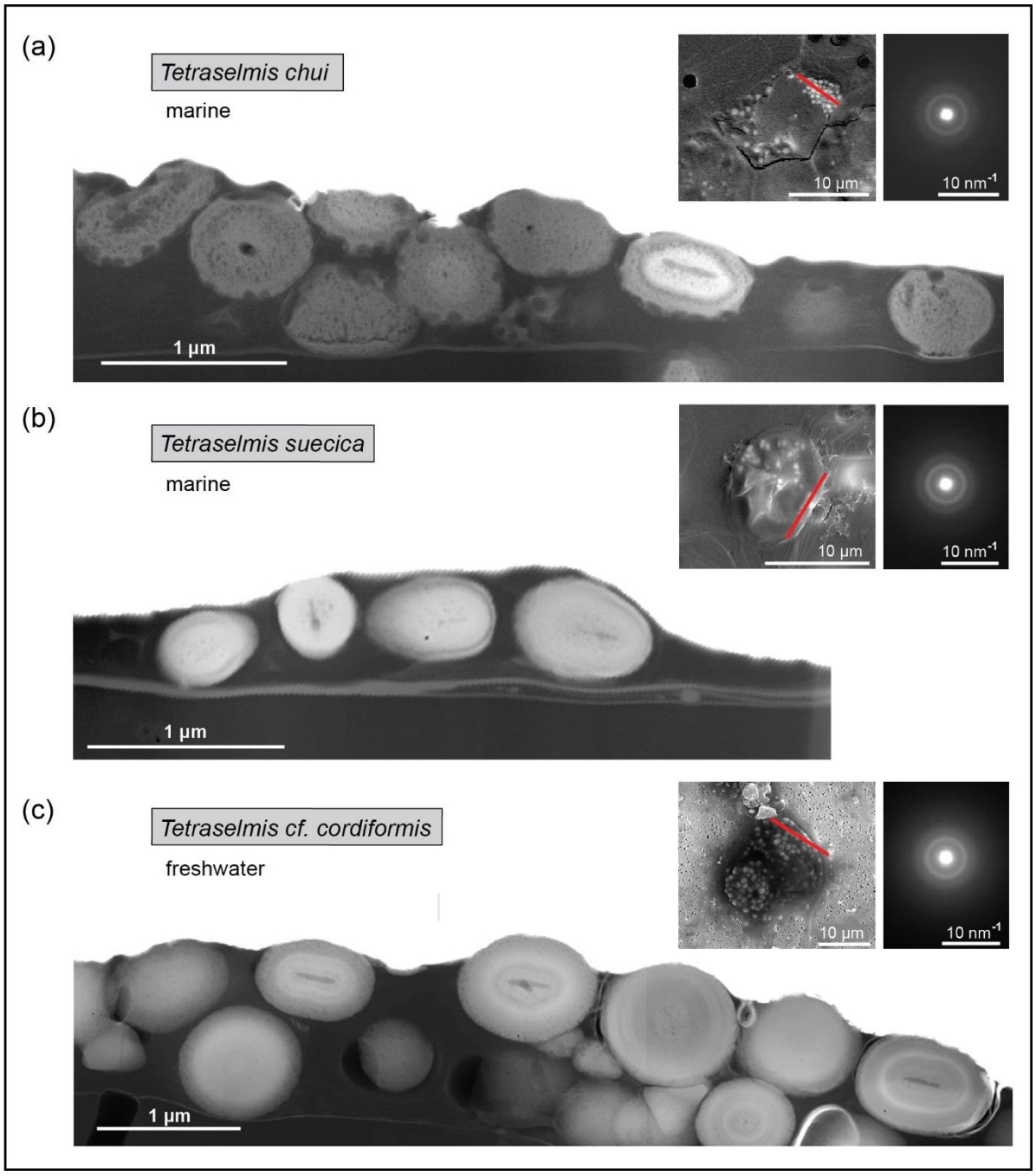

Figure 2: Comparison of FIB-cut sections of cells of three different *Tetraselmis* species (dried samples).

Top left insets: SEM secondary images of the whole cell before FIB preparation indicating the location of the cut with a red line. Top right insets: SAED patterns from a single micropearls of each FIB-cut section (broad diffraction rings are indicative for amorphous material). Bottom TEM-HAADF images: FIB-cut sections through cells of (a) *Tetraselmis chui* (culture sample); (b) *Tetraselmis suecica* (culture

sample); (c) *Tetraselmis cf. cordiformis* (Lake Geneva) (Martignier et al., 2017). Small bubbles inside the micropearls (particularly visible in the marine species) are due to beam damage. The contact between the cell and the filter surface is visible near the bottom in each image.

Micropearls in all four species show strong similarities. They are located inside the organic envelope, are amorphous (Figs 2 and 3) and, except for the sample with pure Ca (*T. contracta* in Fig. 3), they show a distinct internal concentric zonation (Fig 2). In all observed species, the cut sections of micropearls suggest a rod-shaped nucleus in their center (Figs 2 and S3). Moreover, all are most probably highly hydrated given their strong response under the electron beam (results no shown). The dehydration can still be observed for all micropearl types even after more than five months of conservation as dried samples at room temperature.

TEM-EDXS analyses show that the zonation observed in the marine micropearls of *T. chui* and *T. suecica* (Fig. 2 and S4) is due to changes in the Sr/Ca concentration ratios, similarly to the zonation observed in the freshwater micropearls in *Tetraselmis cf. cordiformis* (Martignier et al., 2017). All micropearls within one cell do not necessarily have an identical composition. An example is shown in Fig. 2a, where one micropearl possesses a composition with a higher atomic mass than the rest (lighter grey level in STEM-HAADF image) due to a higher content of Sr. Furthermore, micropearls within one cell display variable zoning patterns (Fig. 2a and 2c).

3.3 TEM-EDXS mapping: location of the micropearls inside a *Tetraselmis contracta* cell

The co-existence of micropearls with other cellular constituents and their respective positions in the cell is shown by a TEM image of a FIB-cut section through a *T. contracta* cell (Fig. 3). The micropearls of this species are large, numerous and nearly exclusively consist of ACC without detectable Sr (Fig. S4). They appear as round to ovoid light grey shapes with smooth surfaces (Fig. 3a). The TEM observation also reveals that most micropearls are not randomly scattered throughout the cell but are located preferentially just under the cell wall.

Although Fig. 3a is difficult to interpret because of the atypical preparation of the sample (simply dried instead of more traditional preparations for TEM-observation such as chemical fixation or cryo-sections), the identification of the visible cellular constituents can still be attempted (Fig. 3b). Side views (lower part of the section) and tangential sections of starch grains (upper part of the section) are visible, as well as a glancing view of the chloroplast, which is reticulated in this species. Although micropearls resemble starch grains at first look, it is quite easy to differentiate them. First, they are generally more rounded than starch grains; secondly, they are not located inside the chloroplast, in particular, they are not associated with the prominent pyrenoid.

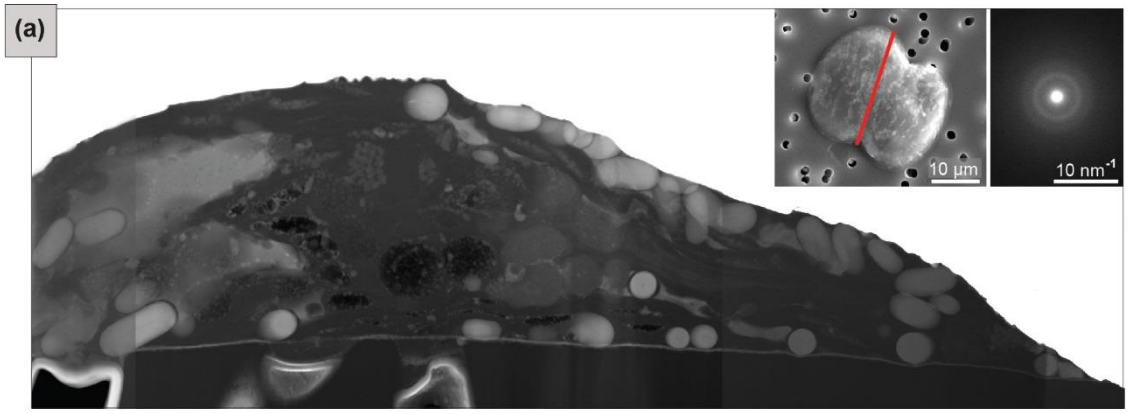
(a)
10 µm
10 nm-1

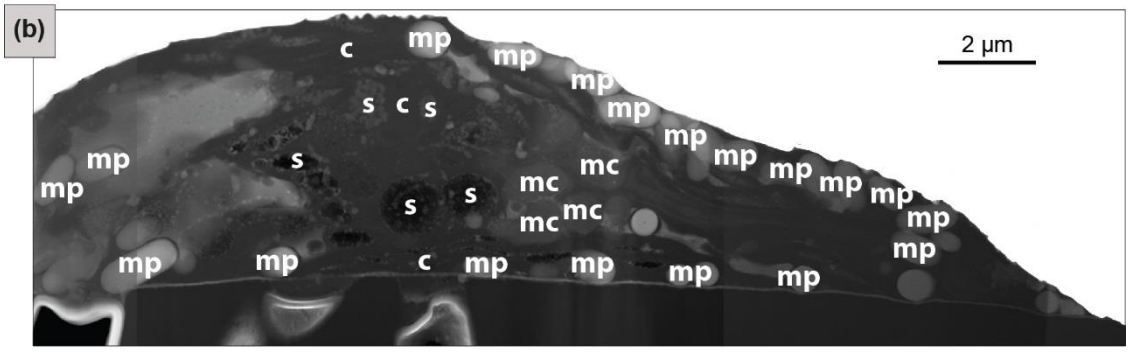
(b)
2 µm
c
mp
s
mc

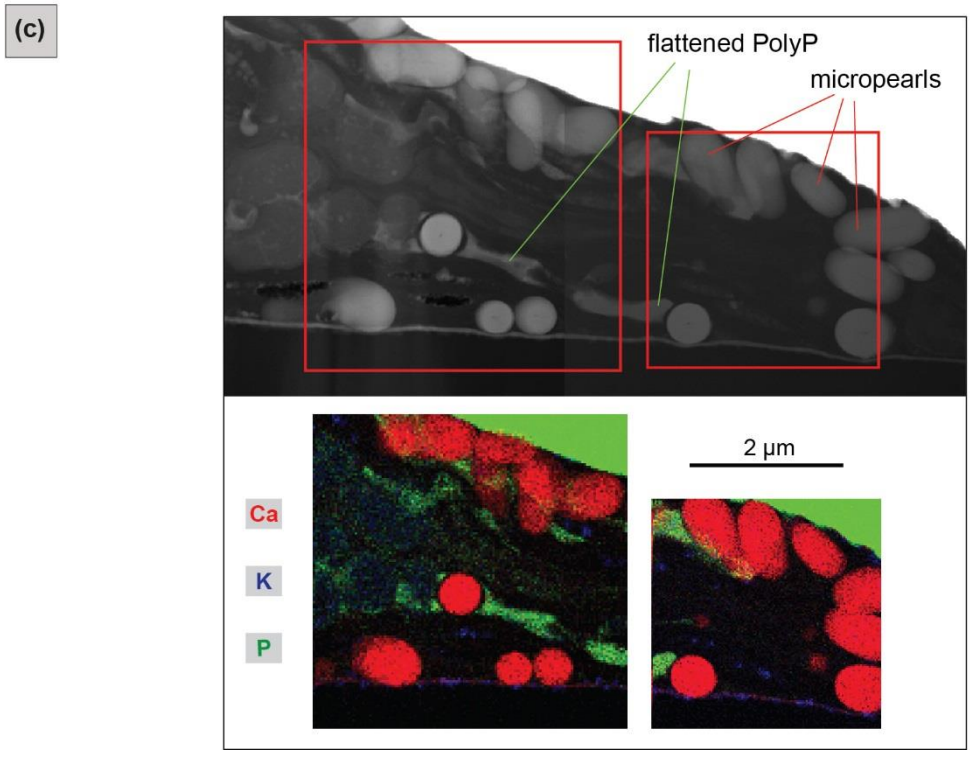
(c)
flattened PolyP
micropearls
2 µm
Ca
K
P

Figure 3: FIB-cut section through a *Tetraselmis contracta* cell (dried sample).

(a) TEM-HAADF image of the whole FIB-cut section. The micropearls show light or medium grey shades, regular round or oval shapes. Top left inset: SEM secondary images of the whole cell before it was cut, with a red line indicating the location of the section. Top right inset: SAED patterns from a single micropearl of this FIB-cut section (diffuse diffraction rings are indicative for amorphous material). (b) Tentative identification of the visible cellular constituents. s: starch grains; c: chloroplast; mp: micropearls; mc: mitochondria.(c) TEM-EDXS mappings - Top image shows the location of the two zones on a TEM-HAADF image of the section. The map shows an RGB image with three superimposed element mappings. Micropearls are mainly composed of Ca, with small quantities of K (and Mg, not shown here). Note that, due the overlap between the P *K* peak and secondary Pt *L* peak, the Pt layer, which was deposited on top of the sample during FIB processing, is also visible in green color.

TEM-EDXS mapping provides compositional information improving the identification of the cellular constituents and organelles visible in the section (Fig. 3c and S5). Micropearls are well visible, based on the high concentration of Ca, with small quantities of K (and sometimes Mg, not shown here). The theca, composed of fused scales, appears as a thin layer between the cell and the filter. Its composition including C, Ca, S and small amounts of K makes it apparent in Fig. 3c (in violet). The theca of these organisms is indeed known to contain 4% of Ca and 6% of S (as sulfate) by weight (Becker et al., 1994, 1998). The two irregular features that are highly enriched in P (in green in Fig. 3c) are identified as being PolyP inclusions, flattened during sample preparation. Finally, the dark grey features, in the center of the section, are probably mitochondrial profiles.

3.4 SEM-EDXS: micropearl composition

The micropearls of most marine species (Fig. 4a) seem to be composed of ACC, with Ca and Sr as cations. This composition is similar to the one measured for micropearls of *T. cordiformis* in Lake Geneva (Martignier et al., 2017). We noted two differences with our previous observations: *T. desikacharyi* forms micropearls containing small amounts of Ba and micropearls of *T. contracta* contain low concentrations of K. However, since growth media had different compositions, these observations need to be taken with care.

Figure 4a compiles the composition of the micropearls for each *Tetraselmis* strain (SEM-EDXS analyses), ranked in increasing order of Sr/Ca median values. Even if low concentrations of K are present in micropearls of *T. contracta*, it was not considered because the element is also present in the surrounding organic matter (Fig. S5), making it impossible to estimate the portion of the measured K that belongs to the micropearls. Magnesium was discarded for the same reason. It should be noted that the size of micropearls is close to or even below the resolution limit of the SEM-EDXS analysis technique. This means that the interaction volume of the electron beam with the sample is often larger than the micropearls themselves and that therefore the technique yields compositions that include the micropearl and the surrounding organic matter or nearby cellular constituents (e.g. polyphosphates).

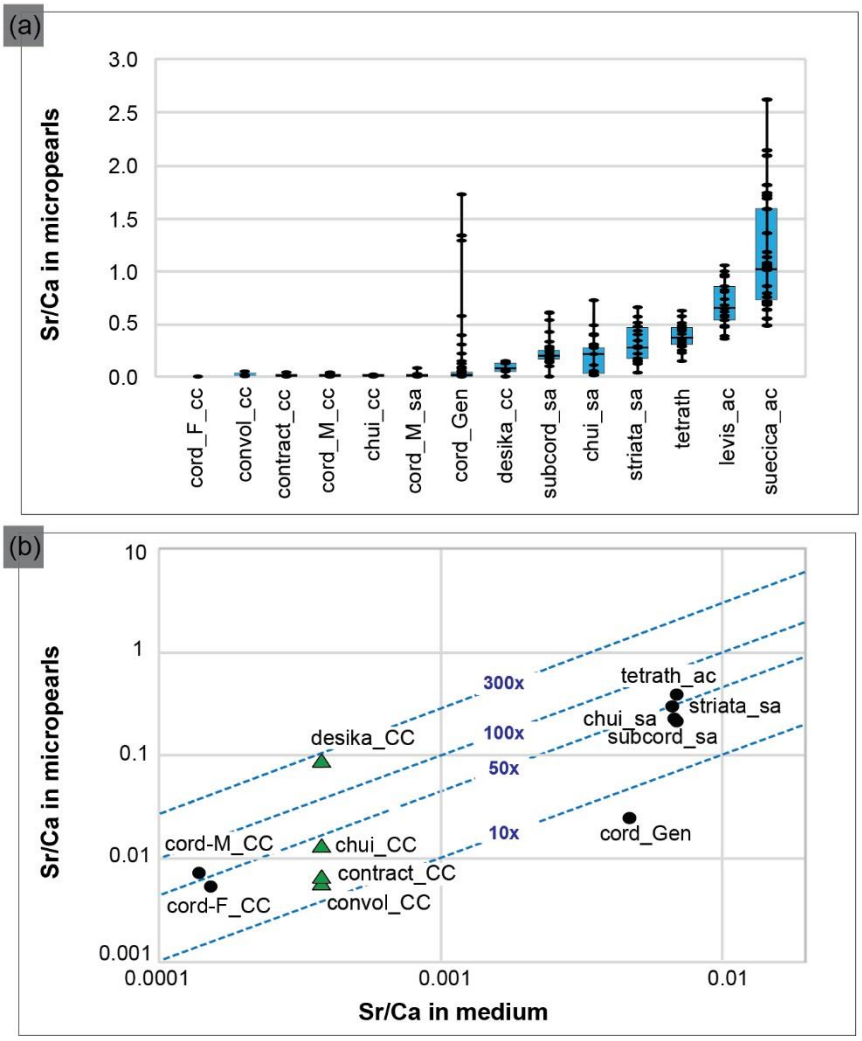

Figure 4: Composition of the *Tetraselmis* micropearls and their relation with the growth media composition.

(a) Distribution of the Sr/Ca ratio for each *Tetraselmis* strain (EDXS analyses), ranked according to the median value of Sr/Ca. At least 20 EDXS analyses were performed on micropearls of each strain. The range between the minimum and maximum data are shown by black lines. The blue boxes represent the 25-75% interquartiles, while the black horizontal line in the boxes shows the median value. (b) Relationship between the composition of the growth media and the composition of the *Tetraselmis* micropearls, expressed as the Sr/Ca ratio. Each point represents the median Sr/Ca ratio measured in each species micropearls, related to the Sr/Ca ratio of the growth medium. The blue dotted lines define the values of the Sr enrichment factor of the micropearls with respect to the medium (10x, 50x, etc.). Ca concentrations of the growth media were calculated, based on media theoretical composition. Green triangles signal four samples grown in the same medium. The abbreviations and characteristics of each strain are indicated in Table 1 while Sr/Ca values appear in Table S2 (for medium) and S3 (for micropearls). Results from *T. cordiformis* from Lake Geneva (cord_Gen) (Martignier et al., 2017) are given as a comparison.

3.5 Sr/Ca ratio in growth media: influence on the micropearl composition

The overall composition of all culture media is rather similar. The culture media concentrations in Sr and Ba are given in Table S2 and represented graphically in Fig. S6. Strontium concentrations range from 3.3 10^{-8} M (freshwater medium SFM) to 7.1 10^{-5} M (seawater SWES medium). All media have lower Sr concentrations than the average seawater (9.1 10^{-5} M). SFM, used to grow *T. cordiformis* - the only freshwater strain under study – has lower Sr concentrations than those measured in Lake Geneva (5.2 10^{-6} M). The molar ratio Sr/Ca has been calculated for seven growth media (Table S2) and 458 micropearls (Table S3) in order to evaluate a possible influence of the medium on the micropearls composition. Differences between the species regarding the micropearls enrichment in Sr compared to their growth medium can be observed. A Sr distribution coefficient (or enrichment factor) was calculated as the molar ratio [(Sr micropearls / Ca micropearls) / (Sr medium / Ca medium)]. These results are synthetized in Fig. 4.

Figure 4b shows the relationship between the Sr/Ca ratio measured in the growth media and in the *Tetraselmis* micropearls. For most of the strains, the Sr enrichment factor of the micropearls with respect to the medium varies between 10 and 100 times (see Table S3 for exact figures), with the notable exception of *T. desikacharyi* (more than 200 times). It is interesting to observe that both strains of *T. chui* - from different geographic origins (Table 1) - have rather similar Sr distribution coefficients (around 30), while the three strains of *T. cordiformis* show slightly different enrichment factors (25 for Lake Geneva water, 33 for Lake Fühlinger and 51 for Münster moat). Broadly speaking, Sr/Ca increases in micropearls together with its increase in the medium. However, the spread in enrichment may be large for a given medium (such as ASP-H for strains of *T.contracta*, *T. convolutae*, *T. chui* and *T. desikacharyi*).

4 Discussion

4.1 Marine micropearls

The discovery of micropearls in marine species of *Tetraselmis* shows that this biomineralization process can take place in organisms growing in waters of different composition, from freshwater, like Lake Geneva, to seawater (Fig. S6). This shows the capacity of these organisms to concentrate Ca and Sr from different external media.

The capacity to form micropearls is clearly not directly related to a specific habitat, since seven *Tetraselmis* species forming micropearls live as phytoplankton in freshwater, marine or brackish waters (Guiry et al., 2017; John et al., 2002), *T. contracta* and *T. desikacharyi* were sampled in the sand, at the bottom of a marine estuary (Marin et al., 1996) or at low tide, and *T. convolutae* is usually observed as a photosymbiont inside a flatworm (Muscatine et al., 1974). Regarding the only two species which did not show micropearls at the time of observation (*T. ascus* and *T. marina*), it is interesting to note that both live as stalked sessile colonies, with motile life-history stages (Norris et al., 1980).

Apart from their elongated shape, "marine" micropearls have similar characteristics to micropearls formed by the freshwater species *T. cordiformis* (Martignier et al., 2017). Micropearls show a range of possible composition for each species (Fig. 4a and Table S3). The elemental ratio seems to be influenced by several parameters, amongst which we identified the composition of the culture medium (Fig. 4b) and the Sr concentrating capacity of each *Tetraselmis* species (e.g. green triangles in Fig.4b). The enrichment capacity displayed by *T. desikacharyi* (219) stands well above all the others (Fig. 4b and Table S3). This could be linked to distinctive morphological features (a six-layered theca, a novel flagellar hair subtype) not found in other strains of *Tetraselmis* (Marin et al., 1996).

4.2 Hints about the formation process of micropearls

The biomineralization process leading to the formation of micropearls seems to start in the same way in all *Tetraselmis* species observed in thin sections (*T. chui, T. contracta, T. cordiformis* and *T. suecica*), with a similar rod-shaped nucleus (Figs 2, 3 and S3). These nuclei could possibly be of organic nature given their darker appearance in the STEM- HAADF images that point to a material of lower atomic mass (Fig. S3).

Internal concentric zones are observed in the micropearls formed by cells grown both in the natural environment and in cultures (Fig. 2). The presence of this concentric pattern, even when the growth media have a stable composition, may indicate that the zonation is not due to changes in the surrounding water/medium composition during micropearl growth, but rather depends on variations in the intracellular fluid composition caused by the biomineralization process itself. In the hypothesis discussed by Thien et al. (2017), it is suggested that the formation of the micropearls results from a combination of a biologically controlled process (preferential intake of specific cations inside the cell) and abiotic physical and chemical mechanisms (mineralization resulting from a non-equilibrium solid-solution growth mechanism, leading to an internal oscillatory zoning). Nevertheless, even that second part of the process does not seem to be purely abiotic, as demonstrated by the long-term amorphous state displayed by micropearls (at least five months, according to our observations). Indeed, such long-term stabilization of ACC generally implies a strong organic control through the integration of additives in the mineral (e.g. certain proteins, polyphosphonates, citrates, amino acids) (Addadi et al., 2003; Cam et al., 2015; Cartwright et al., 2012). ACC, in its pure form, is unstable and will rapidly crystallize into calcite or aragonite (Addadi et al., 2003; Bots et al., 2012; Weiner and Addadi, 2011).

4.3 A new intracellular feature in a well-known genus

Our results (Fig. 1) uncover a strong biomineralization capacity in the genus *Tetraselmis*, confirming that artefacts can be induced by usual biological sample preparation techniques (Martignier et al., 2017) and thus biais observations and even hide some physiological traits in otherwise well-studied organisms. Figure 3c shows that the straightforward sample preparation method used in this study (dried, with no chemical fixation) allows the preservation of the micropearls and can yield interesting data on the composition of the different elements present inside the cell, without any chemical disturbance.

Micropearls represent a new intracellular feature. Their systematic presence in most of the analysed *Tetraselmis* species suggests that they may have a physiological role. A possible explanation could be that micropearls increase the sedimentation rate of cells that shed their flagella upon nitrogen starvation at the end of *Tetraselmis* blooms. An alternative hypothesis is that micropearls represent reserves of Ca for periods when millimolar Ca is not available in the external medium. Indeed, all Chlorodendrophyceae (*Tetraselmis*, *Platymonas* and *Scherffelia*) require a certain concentration of Ca (mM) to survive and multiply (Melkonian, 1982). The evolutionary diversification of this class occurs in the marine habitat, where the Ca concentration is constantly around 10 mM (Table 4.1 in Pilson, 1998). The need for Ca is supported by *T. cordiformis*, the only freshwater species of the genus, occurring only in Ca-rich lakes, with a minimum of 1 mM of Ca (e.g. Lake Geneva (1 mM) or Fühlinger See (2mM)). Calcium is needed to support phototaxis (light-oriented movements) and for the construction and maintenance of the cell coverage (theca, flagellar scales) (Becker et al., 1994; Halldal, 1957). The Sr found in the composition of the micropearls formed by most *Tetraselmis* spp. (Fig. 4) could be transported by the same transporter as Ca. Indeed, *Chlorodendrophyceae* have very efficient light-gated Ca-channels (channelrhodopsins) which are also essential for phototaxis of these flagellates (Govorunova et al., 2013; Halldal, 1957).

4.4 Bioremediation possibilities

The capacity of some organisms to concentrate Sr is of great interest regarding bioremediation. Strontium (^{90}Sr) is one of the radioactive nuclides released in large quantities by accidents such as Chernobyl or Fukushima (Casacuberta et al., 2013) and a major contaminant in wastewater and sludges linked with nuclear activities (Bradley and Frank, 1996). Its relatively long half-life of ~30 years and high water solubility cause persistent water pollutions (Thorpe et al., 2012; Yablokov et al., 2009). The high Sr absorption capacities of several *Tetraselmis* species previously led to their mention as potential candidates for radioactive Sr bioremediation (Fukuda et al., 2014; Li et al., 2006) although the process allowing these microorganisms to concentrate Sr had not yet been investigated . Further studies of micropearl formation processes could therefore lead to new bioremediation techniques. The genus *Tetraselmis* presents the additional advantage of including species living in diverse habitats, which might offer interesting bioremediation applications in different aquatic environments (e.g. freshwater, brackish lakes, open sea, hypersaline lagoons).

5 Conclusions

Until recently, non-skeletal intracellular inclusions of calcium carbonate were considered as nonexistent in unicellular eukaryotes (Raven and Knoll, 2010). After the first observation of at least two micropearl-forming organisms in Lake Geneva (Martignier et al., 2017), the present study shows that these amorphous calcium carbonate (ACC) inclusions are widespread in a common phytoplankton genus (*Tetraselmis*), not only in freshwater, but also in seawater and brackish environments. This newly discovered biomineralization process therefore takes place in media of very different composition but our results suggest that it is similar in all studied species: an oscillatory zoning process that starts from an organic rod-shaped nucleus. Although

frequent in this well-studied genus, these mineral inclusions had been overlooked to date, possibly obliterated by the usual sample preparation techniques for electron microscopy. Thus other microorganisms could have similar capacities and intracellular inclusions of amorphous calcium carbonates may be more widespread than currently known.

Micropearls represent a new intracellular feature. This study shows that they are not randomly distributed in the cell. On the contrary, the distribution of micropearls within the cell seems to be characteristic for each species, and we suggest that this might have a link with the species habitat. Observations of a cell cross-section showed that micropearls are essentially located just under the cell wall, and can be clearly distinguished from other organelles.

In the genus *Tetraselmis*, the biomineralization process leading to the formation of micropearls enables a selective concentration of Sr. The elements concentrated in the micropearls, as well as their degree of enrichment seem to be characteristic for each species. Selecting the species with the highest concentration capacities could be of high interest for bioremediation, especially regarding radioactive Sr contaminations linked with nuclear activities.

Competing interests

The authors declare that they have no conflict of interest.

Acknowledgements

This research was supported by the Société Académique de Genève (Requête 2017/66) and the Ernst and Lucie Schmidheiny Foundation. We thank Mauro Tonolla, Sophie de Respinis and Andreas Bruder (SUPSI) as our collaboration triggered the present research, Barbara Melkonian and the CCAC (University of Cologne) for their help and collaboration, and Maike Lorenz (SAG- University of Göttingen) for culture tips and allowing the analysis of their growth medium. FL is grateful to the Deutsche Forschungsgemeinschaft for funding of the FIB-TEM facilities via the Gottfried-Wilhelm Leibniz program (LA830/14-1). We also thank Stephan Jacquet and Andrew Putnis for advice, as well as Rossana Martini and Camille Thomas for support.

References

Addadi, L., Raz, S. and Weiner, S.: Taking advantage of disorder: Amorphous calcium carbonate and its roles in biomineralization, Adv. Mater., 15, 959–970, doi:10.1002/adma.200300381, 2003.

Asinari di San Marzano, C.-M., Legros, A., Piron, C., Sironval, C., Nyns, E.-J. and Naveau, H. P.: Methane production by anaerobic digestion of algae, in: Energy from biomass: Proceedings of the EC Contractors' Meeting held in Copenhagen, 23--24 June 1981, edited by P. Chartier and W. Palz, Springer Netherlands, Dordrecht, pp. 113–120, 1981.

Azma, M., Mohamed, M. S., Mohamad, R., Rahim, R. A. and Ariff, A. B.: Improvement of medium composition for

heterotrophic cultivation of green microalgae, *Tetraselmis suecica*, using response surface methodology, Biochem. Eng. J., 53, 187–195, doi:10.1016/j.bej.2010.10.010, 2011.

Becker, B., Marin, B. and Melkonian, M.: Structure, composition, and biogenesis of prasinophyte cell coverings, Protoplasma, 181, 233–244, doi:10.1007/BF01666398, 1994.

Becker, B., Melkonian, M. and Kamerling, J. P.: The cell wall (theca) of *Tetraselmis striata* (chlorophyta): macromolecular composition and structural elements of the complex polysaccharides, J. Phycol., 34, 779–787, doi:10.1046/j.1529-8817.1998.340779.x, 1998.

Bots, P., Benning, L. G., Rodriguez-Blanco, J.-D., Roncal-Herrero, T. and Shaw, S.: Mechanistic insights into the crystallization of amorphous calcium carbonate (ACC), Cryst. Growth Des., 12, 3806–3814, doi:10.1021/cg300676b, 2012.

Bradley, D. J., Frank, C. W., and Mikerin, Y.: Nuclear contamination from weapons complexes in the former Soviet Union and the United States, Phys. Today, 49, 40–45, doi:10.1063/1.881495, 1996.

Cam, N., Georgelin, T., Jaber, M., Lambert, J. F. and Benzerara, K.: In vitro synthesis of amorphous Mg-, Ca-, Sr- and Ba-carbonates: What do we learn about intracellular calcification by cyanobacteria?, Geochim. Cosmochim. Acta, 161, 36–49, doi:10.1016/j.gca.2015.04.003, 2015.

Cartwright, J. H. E., Checa, A. G., Gale, J. D. and Sainz-díaz, C. I.: Calcium carbonate polyamorphism and its role in biomineralisation : How many ACCs are there ?, Angew. Chemie Int. Ed., 51, 11960-11970, doi:10.1002/anie.201203125, 2012.

Casacuberta, N., Masqué, P., Garcia-Orellana, J., Garcia-Tenorio, R. and Buesseler, K. O.: ^{90}Sr and ^{89}Sr in seawater off Japan as a consequence of the Fukushima Dai-ichi nuclear accident, Biogeosciences, 10, 3649–3659, doi:10.5194/bg-10-3649-2013, 2013.

Domozych, D. S.: The crystalline cell wall of *Tetraselmis convolutae* (Chlorophyta): a freeze fracture analysis, J. Phycol., 20, 415–418, doi:10.1111/j.0022-3646.1984.00415.x, 1984.

Douglas, A. E.: Uric acid utilization in *Platymonas convolutae* and symbiotic *Convoluta roscoffensis*, J. Mar. Biol. Assoc. United Kingdom, 63, 435-447, doi:10.1017/S0025315400070788, 1983.

Fukuda, S. ya, Iwamoto, K., Atsumi, M., Yokoyama, A., Nakayama, T., Ishida, K. ichiro, Inouye, I. and Shiraiwa, Y.: Global searches for microalgae and aquatic plants that can eliminate radioactive cesium, iodine and strontium from the radio-polluted aquatic environment: A bioremediation strategy, J. Plant Res., 127, 79–89, doi:10.1007/s10265-013-0596-9, 2014.

Gooday, G. W.: A physiological comparison of the symbiotic alga platymonas convolutae and its free-living relatives, J. Mar. Biol. Assoc. United Kingdom, 50, 199-208, doi:10.1017/S0025315400000710, 1970.

Govorunova, E. G., Sineshchekov, O. A., Li, H., Janz, R. and Spudich, J. L.: Characterization of a highly efficient blue-shifted channelrhodopsin from the marine alga platymonas subcordiformis, J. Biol. Chem., 288, 29911–29922, doi:10.1074/jbc.M113.505495, 2013.

Grierson, S., Strezov, V., Bray, S., Mummacari, R., Danh, L. T. and Foster, N.: Assessment of bio-oil extraction from *Tetraselmis chui* microalgae comparing supercritical CO_2, solvent extraction, and thermal processing, Energ. Fuels, 26, pp.

248–255, doi:10.1021/ef2011222, 2012.

Guiry, M. D. and Guiry, G. M.: AlgaeBase, World-wide Electron. Publ. Natl. Univ. Ireland, Galw. [online] Available from: http://www.algaebase.org, 2017.

Halldal, P.: Importance of calcium and magnesium ions in phototaxis of motile green algae, Nature, 179, 215–216, doi:10.1038/179215b0, 1957.

Hemaiswarya, S., Raja, R., Ravi Kumar, R., Ganesan, V. and Anbazhagan, C.: Microalgae: A sustainable feed source for aquaculture, World J. Microbiol. Biotechnol., 27, 1737–1746, doi:10.1007/s11274-010-0632-z, 2011.

Jaquet, J. M., Nirel, P. and Martignier, A.: Preliminary investigations on picoplankton-related precipitation of alkaline-earth metal carbonates in meso-oligotrophic lake Geneva (Switzerland), J. Limnol., 72, 592–605, doi:10.4081/jlimnol.2013.e50, 2013.

John, D. M., Whitton, B. A., Brook, A. J.:The freshwater algal flora of the British Isles: An identification guide to freshwater and terrestrial algae, Natural History Museum (London) and British Phycological Society, Cambridge University Press, 2002.

Kirst, G. O.: Ion composition of unicellular marine and fresh-water algae, with special reference to *Platymonas subcordiformis* cultivated in media with different osmotic strengths, Oecologia, 28, 177–189, doi:10.1007/BF00345253, 1977.

Li, M., Xie, X., Xue, R. and Liu, Z.: Effects of strontium-induced stress on marine microalgae*Platymonas subcordiformis* (Chlorophyta: Volvocales), Chinese J. Oceanol. Limnol., 24, 154–160, doi:10.1007/BF02842815, 2006.

Lim, D. K. Y., Garg, S., Timmins, M., Zhang, E. S. B., Thomas-Hall, S. R., Schuhmann, H., Li, Y. and Schenk, P. M.: Isolation and evaluation of oil-producing microalgae from subtropical coastal and brackish waters, PLoS One, 7, doi:10.1371/journal.pone.0040751, 2012.

Lu, L., Wang, J., Yang, G., Zhu, B. and Pan, K.: Biomass and nutrient productivities of *Tetraselmis chuii* under mixotrophic culture conditions with various C:N ratios, Chinese J. Oceanol. Limnol., 35, 303–312, doi:10.1007/s00343-016-5299-3, 2017.

Manton, I. and Parke, M.: Observations on the structure of two species of *Platymonas* with special reference to flagellar scales and the mode of origin of the theca, J. Mar. Biol. Assoc. United Kingdom, 45, 743–754, doi:10.1017/S0025315400016568, 1965.

Marin, B., Matzke, C. and Melkonian, M.: Flagellar hairs of *Tetraselmis* (Prasinophyceae): Ultrastructural types and intrageneric variation, Phycologia, 32, 213–222, doi:10.2216/i0031-8884-32-3-213.1, 1993.

Marin, B., Hoef-Emden, K. and Melkonian, M. .: Light and electron microscope observations on *Tetraselmis desikacharyi* sp. nov.(Chlorodendrales, Chlorophyta), Nov. Hedwigia, 112, 461–475, 1996.

Martignier, A., Pacton, M., Filella, M., Jaquet, J. M., Barja, F., Pollok, K., Langenhorst, F., Lavigne, S., Guagliardo, P., Kilburn, M. R., Thomas, C., Martini, R. and Ariztegui, D.: Intracellular amorphous carbonates uncover a new biomineralization process in eukaryotes, Geobiology, 15, 240–253, doi:10.1111/gbi.12213, 2017.

Melkonian, M.: An ultrastructural study of the flagellate *Tetraselmis cordiformis* stein (Chlorophyceae) with emphasis on the flagellar apparatus, Protoplasma, 98, 139–151, doi:10.1007/BF01676667, 1979.

Melkonian, M.: Effect of divalent cations on flagellar scales in the green flagellate *Tetraselmis cordiformis*, Protoplasma, 111,

221–233, doi:10.1007/BF01281970, 1982.

Montero, M. F., Aristizábal, M. and García Reina, G.: Isolation of high-lipid content strains of the marine microalga *Tetraselmis suecica* for biodiesel production by flow cytometry and single-cell sorting, J. Appl. Phycol., 23, 1053–1057, doi:10.1007/s10811-010-9623-6, 2011.

Muscatine, L., Boyle, J. E. and Smith, D. C.: Symbiosis of the acoel flatworm *Convoluta roscoffensis* with the alga *Platymonas convolutae*, Proc. R. Soc. B, 187, 221–234, doi:10.1098/rspb.1974.0071, 1974.

Norris, R. E. ., Hori, T. . and Chihara, M.: Revision of the genus *Tetraselmis* (Class Prasinophyceae), Bot. Mag. Tokyo, 93, 317–339, doi:10.1007/BF02488737, 1980.

Park, J. E. and Hur, S.-B.: Optimum culture condition of four species of microalgae as live food from China, J. Aquac., 13, 107–117, 2000.

Parke, M. and Manton, I.: The specific identity of the algal symbiont in *Convoluta roscoffensis*, J. Mar. Biol. Assoc. United Kingdom, 47, 445–464, doi:10.1017/S002531540005654X, 1967.

Pilson, M. E. Q.: An introduction to the chemistry of the sea, 2nd ed., Cambridge University Press, 1998.

Raven, J. A. and Knoll, A. H.: Non-skeletal biomineralization by eukaryotes: Matters of moment and gravity, Geomicrobiol. J., 27, 572–584, doi:10.1080/01490451003702990, 2010.

Regan, D. L.: Other micro-algae, in: Micro-Algal Biotechnology, edited by M. A. Borowitzka and L. J. Borowitzka, Cambridge University Press, pp. 135-150, 1988.

Salisbury, J.L., Baron, A., Surek, B., Melkonian, M.: c, J. Cell Biol., 99, 962-970, doi: 10.1083/jcb.99.3.962, 1984.

Stein, F. R.: Der Organismus der Infusionstiere, III, 1. Hälfte Flagellaten, edited by Engelmann, Leipzig, 1878.

Thien, B., Martignier, A., Jaquet, J. M. and Filella, M.: Linking environmental observations and solid solution thermodynamic modeling: The case of Ba- and Sr-rich micropearls in Lake Geneva, Pure Appl. Chem., 89, 645–652, doi:10.1515/pac-2017-0205, 2017.

Thorpe, C. L., Lloyd, J. R., Law, G. T. W., Burke, I. T., Shaw, S., Bryan, N. D. and Morris, K.: Strontium sorption and precipitation behaviour during bioreduction in nitrate impacted sediments, Chem. Geol., 306–307, 114–122, doi:10.1016/j.chemgeo.2012.03.001, 2012.

Trench, R. K.: The cell biology of plant-animal symbiosis, Ann. Rev. Plant Physiol., 30, 485–531, doi:10.1146/annurev.pp.30.060179.002413, 1979.

Venn, A. A., Loram, J. E. and Douglas, A. E.: Photosynthetic symbioses in animals, J. Exp. Bot., 59, 1069–1080, doi:10.1093/jxb/erm328, 2008.

Wei, L., Huang, X. and Huang, Z.: Temperature effects on lipid properties of microalgae *Tetraselmis subcordiformis* and *Nannochloropsis oculata* as biofuel resources, Chinese J. Oceanol. Limnol., 33, 99–106, doi:10.1007/s00343-015-3346-0, 2015.

Weiner, S. and Addadi, L.: Crystallization pathways in biomineralization, Ann. Rev. Mater. Res., 41, 21–40, doi:10.1146/annurev-matsci-062910-095803, 2011.

Yablokov, A. V., Nesterenko, V. B., Nesterenko, A. V. and Sherman, J. D.: Chernobyl : Consequences of the catastrophe for people and the environment, Published by Blackwell Pub. on behalf of the New York Academy of Sciences., 2009.
Zittelli, G. C., Rodolfi, L., Biondi, N. and Tredici, M. R.: Productivity and photosynthetic efficiency of outdoor cultures of *Tetraselmis suecica* in annular columns, J. Aquac., 261, 932–943, doi:10.1016/j.aquaculture.2006.08.011, 2006.

	origin of the sample	approx. micropearl size	culture medium	provider **strain n°**	abbreviation
Chlamydomonas					
C. reinhardtii	**freshwater** France	no micropearls observed	L-C	TCC 778	-
C. Intermedia	**freshwater** France, Lake Geneva	no micropearls observed	L-C	TCC 113	-
Tetraselmis					
T. ascus	**marine** Spain, Canary Islands, St Cristobal	no micropearls observed	ASP-12	CCAC 3902	-
T. chui	**marine** Germany, Heligoland	0.7 µm length	ASP-H	CCAC 0014	chui_sa
	marine Scotland, Millport, Clyde estuary	0.7 µm length	1/2 SWEg Ag	SAG 8.6	chui_cc
T. contracta	**marine** France, Bretagne, Batz island	1.2 µm length	ASP-H	CCAC 1405	contract_cc
T. convolutae	**marine** (symbiotic in flatworm) France, Bretagne, Batz island	0.8 µm length	ASP-H	CCAC 0100	convol_cc
T. cordiformis	**freshwater** Germany, Cologne, Lake Fühlinger	1 µm diameter	SFM	CCAC 0051	cord-F_cc
	freshwater Germany, Münster, castle ditch	1 µm diameter	Waris - H	CCAC 0579B	cord-M_cc
	freshwater Strain 0579B obtained from CCAC	1 µm diameter	Diat	SAG 26.82	cord-M_sa
T. desikacharyi	**marine** France, Batz island, Rochigou	0.9 µm length	ASP-H	CCAC 0029	desika_cc
T. levis	**marine** France, Saint-Gilles-Croix-de-Vie	0.6 µm length	ES	AC 257	levis_ac
T. marina	**marine** Strain CA5, from L. Provasoli	no micropearls observed	Porph Ag	SAG 202.8	-
T. striata	**marine** UK, N-Wales, Conway	0.6 µm length	SWES Ag	SAG 41.85	striata_sa
T. subcordiformis	**marine** USA, Connecticut, New Haven	0.4 µm length	Porph Ag	SAG 161-1a	subcord_sa
T. suecica	**marine** UK, Plymouth	0.7 µm length	ES	AC 254	suecica_ac
T. tetrathele	**marine** -	0.9 µm length	ES	AC 261	tetrah_ac
T. tetrathele	**brackish** UK	0.9 µm length	Porph Ag	SAG 161-2c	tetrath_sa

Table 1: Specific information for each species and their culture conditions.

Providers: CCAC: Culture Collection of Algae at the University of Cologne (Germany) - www.ccac.uni-koeln.de ; SAG: Sammlung von Algenkulturen at the University of Göttingen (Germany) - https://www.uni-goettingen.de/de/184982.html ; AC: Algobank - culture collection of microalgea of the University of Caen (France) - www.unicaen.fr/algobank; TCC: Thonon Culture Collection of the CARRTEL of Thonon-les-Bains (France) - www6.inra.fr/carrtel-collection. All culture media compositions are indicated on the websites (detailed addresses in Table S1).

Supplementary Materials

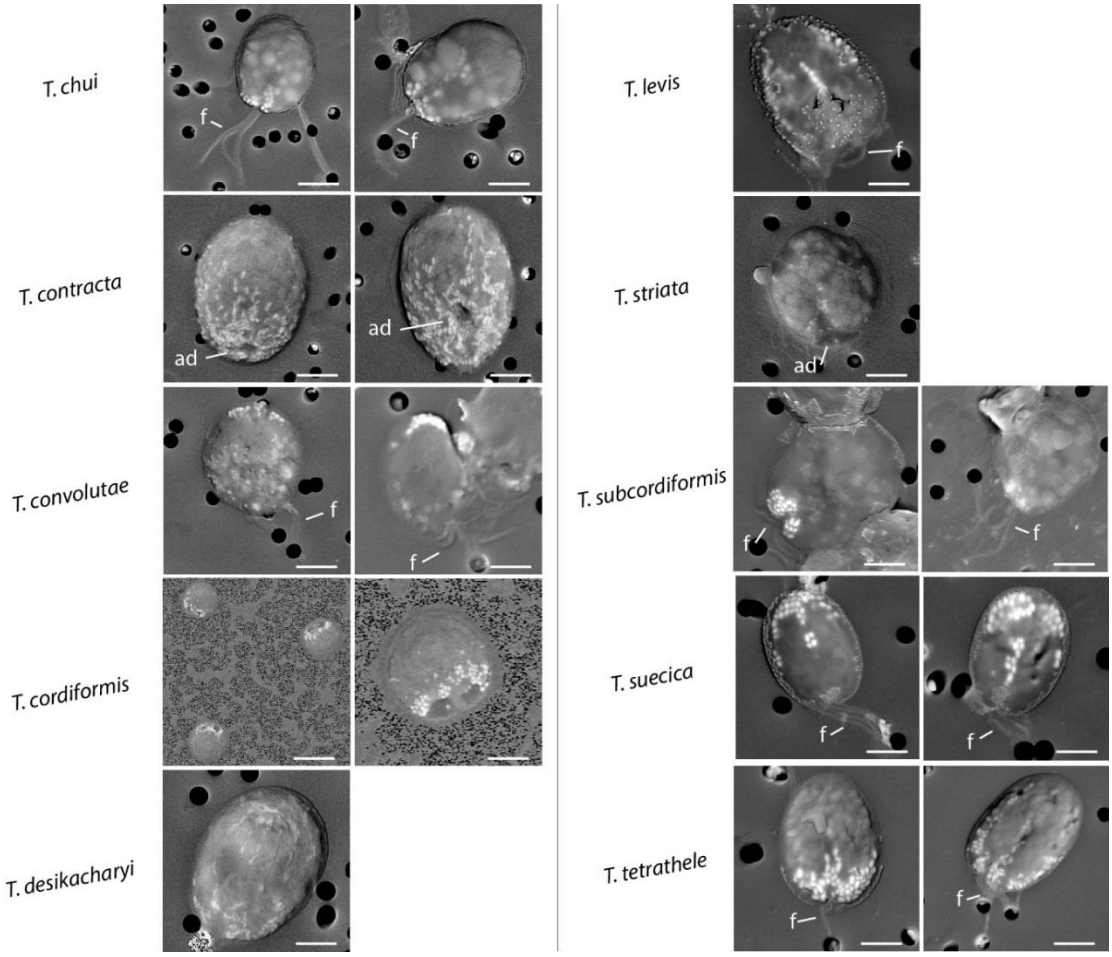

Figure S1: SEM images providing an overview of the micropearl location in *Tetraselmis* species.

Backscattered electron images of dried samples. The micropearls appear in white or light grey against the darker organic matter. The larger and slightly darker inclusions are polyphosphate (observed here in *T. chui*, *T. convolutae*, *T. striata*, *T. subcordiformis*). Pores of the filters are visible as black circles in the background (0.2/1 or 2 micrometers of diameter). The location of the micropearls is linked to the observation of flagella (f) or of the apical depression (ad). In *T. cordiformis*, the two contractile vacuoles are clearly visible and are located at the apical side of the cell. Finally, the orientation of *T. desikacharyi* stays completely uncertain, although similar observations in *T. convolutae* seem to indicate that the iron oxide minerals (in white) are formed around the (missing) flagella. Scale bars: 5µm.

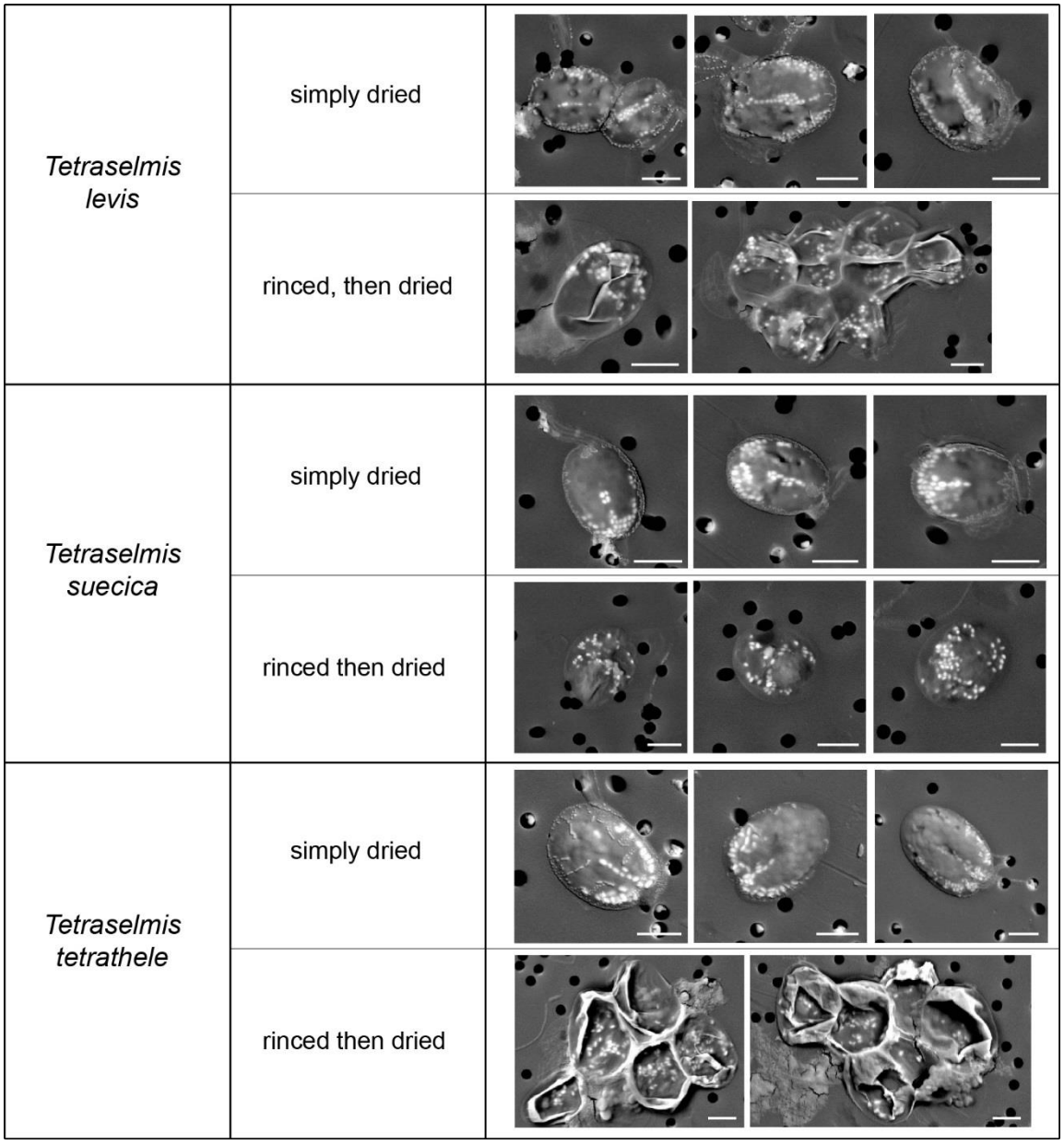

Figure S2: SEM images illustrating how rinsing with MilliQ water disrupts the micropearl distribution pattern inside the cell.

Backscattered electron images of dried samples. The micropearls appear in white or light grey against the darker organic matter. Each culture was sampled at the same time, but prepared in two different ways: either simply dried on a filter, either rinsed shortly with MilliQ water and then dried on a filter. The micropearls' distribution inside the cell is not preserved when the sample is rinsed. Scale bars: 5μm.

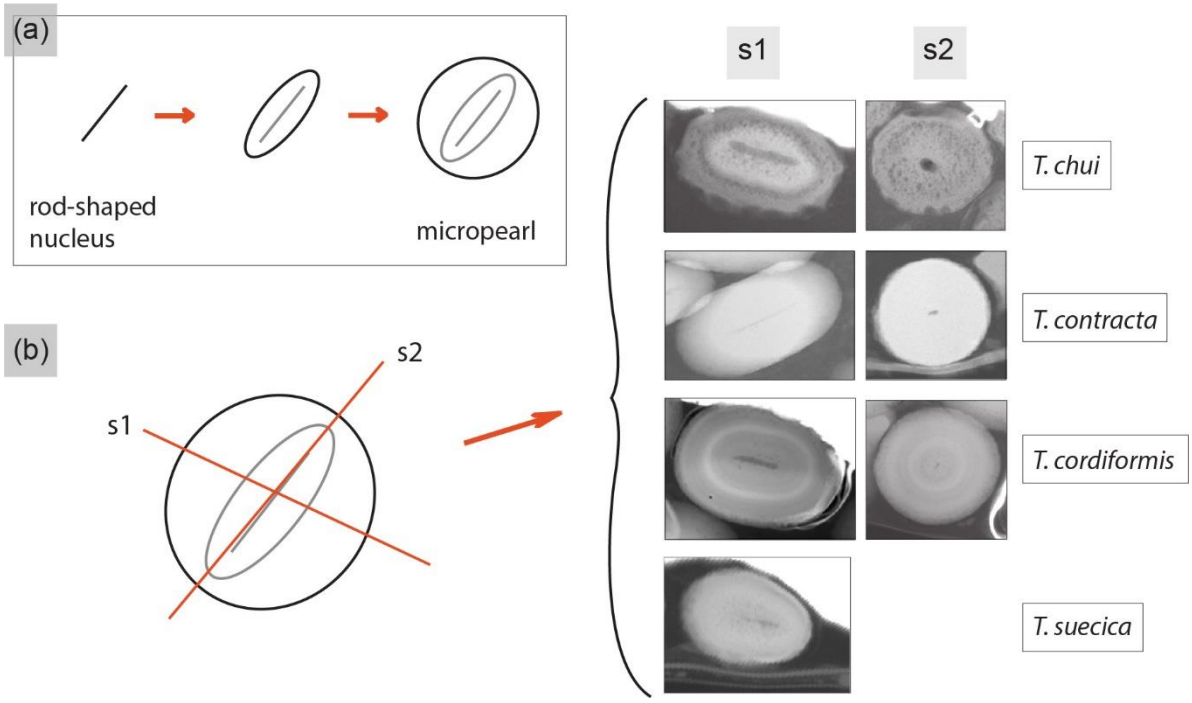

Figure S3: Nucleus shape interpretation for micropearls formed by *Tetraselmis* species.

Cells from algal cultures except *T.*cf *cordiformis*, which was sampled in Lake Geneva (dried samples). (a) Diagram of a possible formation process starting from a rod-shaped nucleus. (b) TEM HAADF images of FIB-cut sections in micropearls formed by *Tetraselmis* species, corresponding to the cross-sections located on the left hand-side drawing. The micropearls measure between 0.7 (*T. chui*) to 1.2 μm (*T. contracta*) in length.

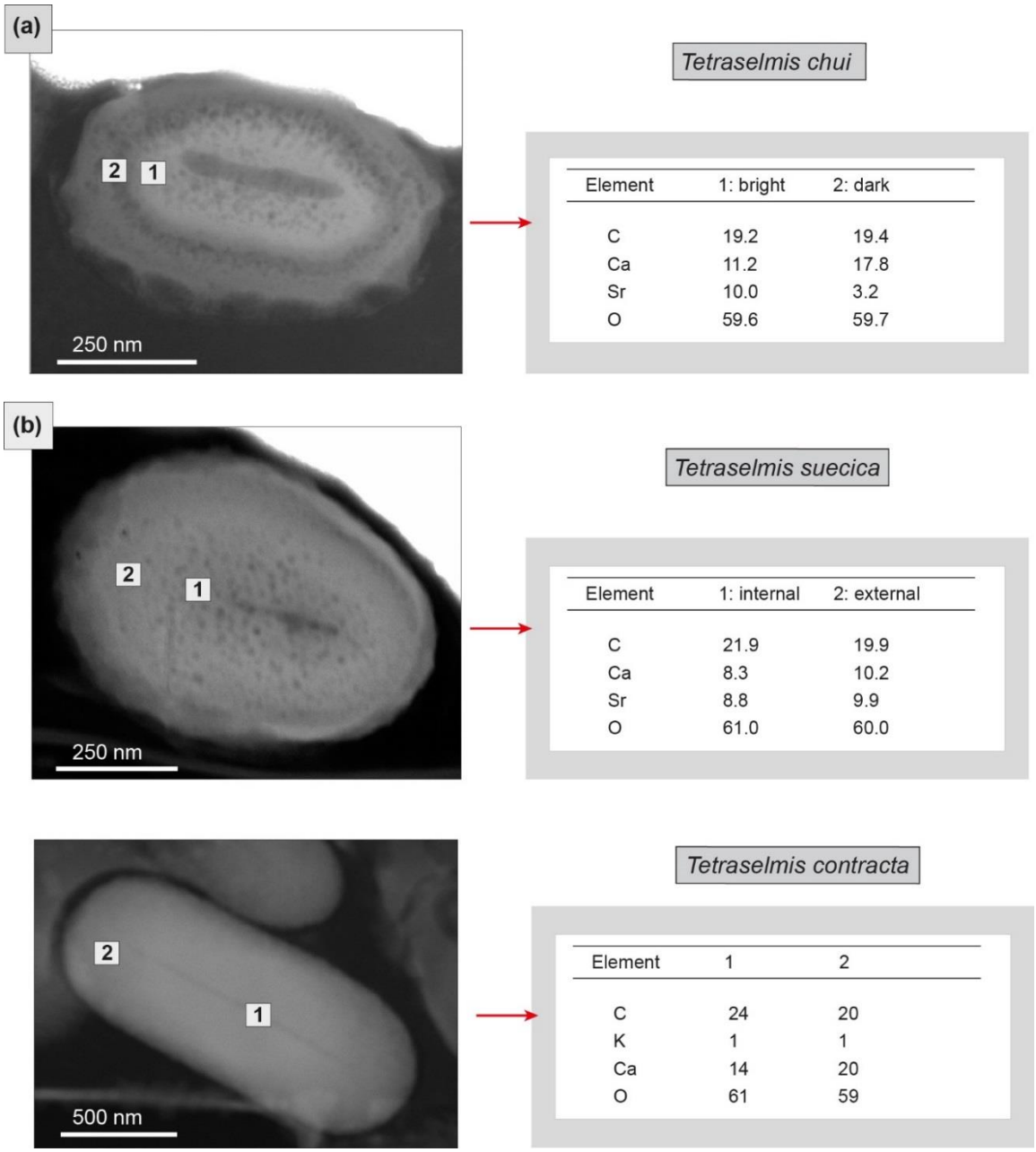

Figure S4: TEM-EDXS analyses of *T. contracta, T. chui and T. suecica* micropearls composition.

STEM – HAADF image. The location of the EDXS analyses (right hand-side table) is indicated by the corresponding numbers. Results are normalized to 100 at%. O is calculated stoichiometrically based on the cation concentrations. Notice the low but significant presence of K in the micropearl composition of *T. contracta*. However its analysis n°1 does not fulfil carbonate stoichiometry, which may be due to the excess C from organic matter. Note that the calculation mode for the analyses presented in this figure differ from those presented in the rest of the manuscript, as C and O are included in the composition.

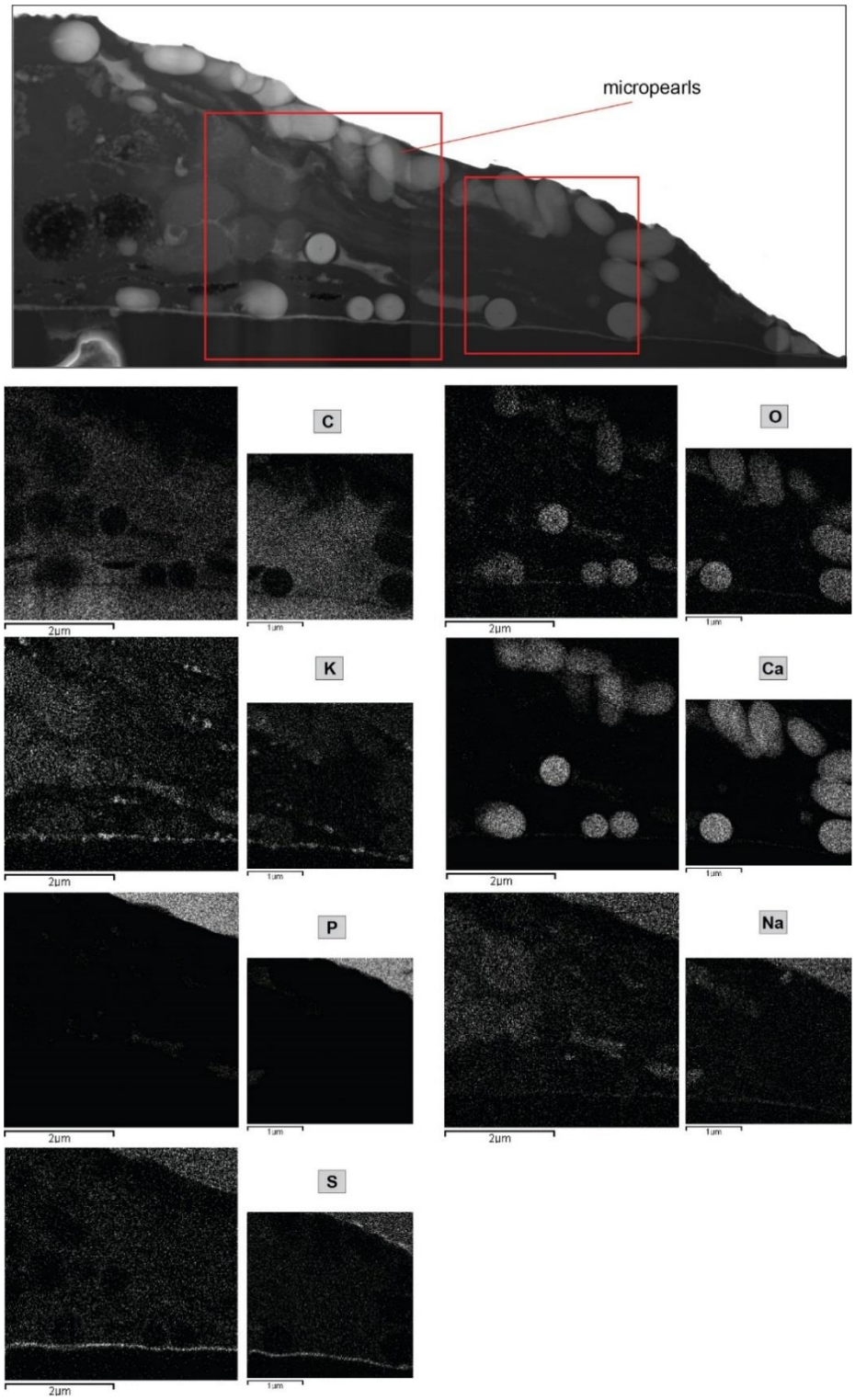

Figure S5: TEM-EDXS mapping results performed on a FIB-cut section through a *Tetraselmis contracta* cell (dried culture sample).

Top image shows the location of the two mappings on a TEM-HAADF image of the section. The maps show the concentration of the different elements: the lighter the color, the more the element is concentrated in that point. Micropearls are mainly composed of Ca, with small quantities of K (and Mg, not shown here). The ACC appears to contain less carbon than the surrounding organic matter, because calcite is known to contain 12 wt% of carbon while the biomass contains 40-50%. Note that, due to the overlap between the P *K* peak and secondary Pt *L* peak, the Pt which was deposited on top of the sample during FIB processing is also visible in green.

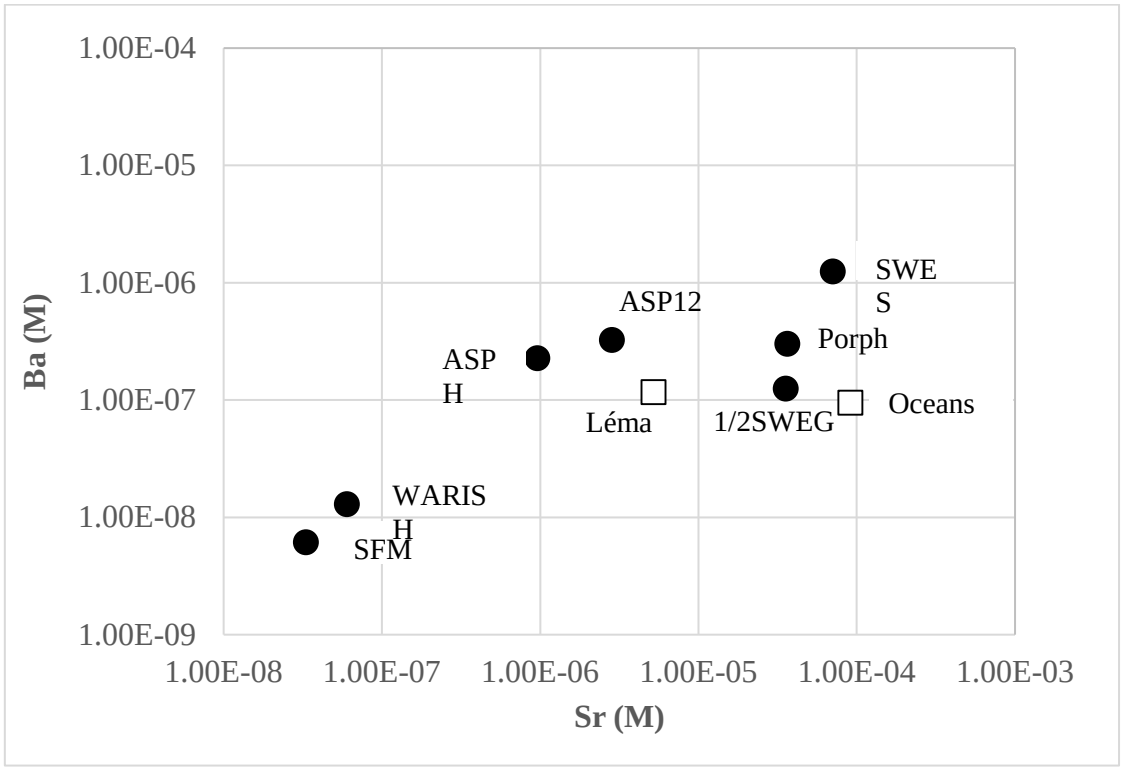

Figure S6: Growth media concentrations in Sr and Ba.

Black dots: culture media; white squares: natural waters. Lake Geneva (Jaquet et al. 2013) and oceans (Bruland and Lohan, 2003). Notice the log scale.

References:

Bruland, K.W. and Lohan, M.C.: Controls of Trace Metals in Seawater, In: Treatise on Geochemistry, Volume 6. Elsevier, chapter 6.02, 2003.

Martignier, A., Pacton, M., Filella, M., Jaquet, J. M., Barja, F., Pollok, K., Langenhorst, F., Lavigne, S., Guagliardo, P., Kilburn, M. R., Thomas, C., Martini, R. and Ariztegui, D.: Intracellular amorphous carbonates uncover a new biomineralization process in eukaryotes, Geobiology, 15, 240–253, doi:10.1111/gbi.12213, 2017.

Provider	Internet address
CCAC Culture Collection of Algae at the University of Cologne	http://www.ccac.uni-koeln.de/sidebar/growth-media/
SAG Sammlung von Algenkulturen at the University of Göttingen	http://www.uni-goettingen.de/en/list+of+media+and+recipes/186449.html
AC Algobank Caen University	https://www.unicaen.fr/algobank/infos/recettes.html

Table S1: Sources for the composition of culture media.

	algal collection	dilution	Sr88(LR) [ppb]	Ba138(L) [ppb]	Sr [M]	Ba [M]	Sr /Ca
Blank - MilliQ_Ge	-		2,48	2,71			
Blank - H2O	CCAC		0,68	0,37			
Blank - MilliQ	SAG		23,43	4,14			
Temoin_10ppb	-		9,89	9,83			
Temoin_100ppb	-		99	103,06			
Waris_H	CCAC		5,27	1,77	6.01E-08	1.29E-08	**1.42E-04**
SFM	CCAC		2,91	0,84	3.32E-08	6.12E-09	**1.58E-04**
1_2_SWEG	SAG		3122,6	17,11	3.56E-05	1.25E-07	**6.77E-03**
ASP-12	CCAC	100	249,47	44,42	2.85E-06	3.23E-07	**2.71E-04**
ASP-H	CCAC	100	84,22	31,09	9.61E-07	2.26E-07	**3.84E-04**
Porph	SAG	100	3196,8	41,38	3.65E-05	3.01E-07	**6.93E-03**
SWES	SAG	100	6201,34	170,84	7.08E-05	1.24E-06	**6.72E-03**

Table S2: Concentration of Sr and Ba measured in the growth media.

Sr and Ba: ICP-MS data.Ca concentrations were calculated based on the media theoretical composition. CCAC: Culture Collection of Algae at the University of Cologne (Germany); SAG: Sammlung von Algenkulturen of the University of Göttingen (Germany); Algobank: culture collection of microalgea of the University of Caen (France). Media ES (Algobank) and Diat (SAG) were not available for analysis.

	cord-F_cc	convol_cc	contract_cc	cord-M_cc	chui_cc	cord_M_sa	cord_Gen	desika_cc	subcord_sa	chui_sa	striata_sa	tetrah	levis_ac	suecica_ac	
Ca norm	0.99	0.99	0.99	0.99	0.99	0.98	0.93	0.90	0.83	0.85	0.77	0.72	0.60	0.49	
Sr norm	0.01	0.01	0.01	0.01	0.01	0.02	0.07	0.08	0.17	0.15	0.23	0.28	0.40	0.51	
Sr/Ca															Total
N	48	22	23	68	48	21	70	22	42	31	38	33	29	33	528
Min	0.000	0.000	0.000	0.000	0.000	0.000	0.000	0.000	0.000	0.013	0.042	0.161	0.374	0.490	
Max	0.013	0.050	0.015	0.046	0.025	0.087	1.728	0.154	0.611	0.734	0.667	0.631	1.060	2.620	
Mean	0.005	0.015	0.006	0.008	0.013	0.019	0.118	0.090	0.218	0.199	0.320	0.391	0.701	1.152	
Std. error	0.0005	0.0037	0.0010	0.0008	0.0009	0.0041	0.0369	0.0096	0.0183	0.0306	0.0263	0.0181	0.0394	0.0925	
Stand. dev	0.0038	0.0175	0.0046	0.0067	0.0064	0.0190	0.3090	0.0449	0.1187	0.1705	0.1618	0.1042	0.2120	0.5311	
Median	**0.005**	**0.006**	**0.006**	**0.007**	**0.013**	**0.015**	**0.025**	**0.085**	**0.208**	**0.225**	**0.290**	**0.376**	**0.661**	**1.030**	
25 prcntil	0.001	0.000	0.002	0.004	0.010	0.010	0.004	0.060	0.178	0.040	0.179	0.320	0.545	0.735	
75 prcntil	0.008	0.030	0.010	0.011	0.018	0.024	0.057	0.133	0.260	0.290	0.476	0.469	0.902	1.465	
Coeff. var	73	116	73	81	49	98	262	50	54	85	51	27	30	46	
Medium	SFM	**ASP-H**	**ASP-H**	**Waris-H**	**ASP-H**	Diat	**Lake water**	**ASP-H**	**Porph Ag**	**1/2 SWEg Ag**	**SWES Ag**	**Porp Ag**	ES	ES	
Sr/Ca med	1.58E-04	3.84E-04	3.84E-04	1.42E-04	3.84E-04		4.73E-03	3.84E-04	6.93E-03	6.77E-03	6.72E-03	6.93E-03			
Sr/Ca mp	5.23E-03	5.50E-03	6.28E-03	7.23E-03	1.25E-02	1.48E-02	2.41E-02	8.43E-02	2.08E-01	2.25E-01	2.90E-01	3.76E-01	6.61E-01	1.03E+00	
Enrichment	**33**	**14**	**16**	**51**	**33**		25	**219**	**30**	**33**	**43**	**54**			

Table S3: Composition statistics for micropearls formed by *Tetraselmis* species.

Composition statistics for 13 Tetraselmis strains micropearls. Values from Lake Geneva (labelled cord_Gen; *Martignier et al. 2017*) are given for comparison. Ca norm, Sr norm: values normalized to 1.0. In the lower part of the table, Sr/Ca ratios of the micropearls (mp) are compared to the ratios in their growth medium (med). Enrichment = [(Sr/Ca mp) / (Sr/Ca med)].

References:

Martignier, A., Pacton, M., Filella, M., Jaquet, J. M., Barja, F., Pollok, K., Langenhorst, F., Lavigne, S., Guagliardo, P., Kilburn, M. R., Thomas, C., Martini, R. and Ariztegui, D.: Intracellular amorphous carbonates uncover a new biomineralization process in eukaryotes, Geobiology, 15, 240–253, doi:10.1111/gbi.12213, 2017.